Electrochemical surface-enhanced Raman spectroscopy of nanostructures

De-Yin Wu, Jian-Feng Li, Bin Ren* and Zhong-Qun Tian*

Received 19th March 2008
First published as an Advance Article on the web 3rd April 2008
DOI: 10.1039/b707872m

This *tutorial review* first describes the early history of SERS as the first SERS spectra were obtained from an electrochemical cell, which led to the discovery of the SERS effect in mid-1970s. Up to date, over 500 papers have been published on various aspects of SERS from electrochemical systems. We then highlight important features of electrochemical SERS (EC-SERS). There are two distinctively different properties of electric fields, the electromagnetic field and static electrochemical field, co-existing in electrochemical systems with various nanostructures. Both chemical and physical enhancements can be influenced to some extent by applying an electrode potential, which makes EC-SERS one of the most complicated systems in SERS. Great efforts have been made to comprehensively understand SERS and analyze EC-SERS spectra on the basis of the chemical and physical enhancement mechanisms in order to provide meaningful information for revealing the mechanisms of electrochemical adsorption and reaction. The EC-SERS experiments and applications are then discussed from preparation of nanostructured electrodes to investigation of SERS mechanisms and from characterization of adsorption configuration to elucidation of electrochemical reaction mechanisms. Finally, prospective developments of EC-SERS in substrates, methods and theory are discussed.

1 History of electrochemical surface-enhanced Raman spectroscopy

The first surface-enhanced Raman scattering (SERS) spectra were obtained from an electrochemical cell, which led to the discovery of the SERS effect in mid-1970s. In looking back, one may not be too surprised about why the SERS research was initiated from an electrochemical system, as electrochemistry was just in the transition stage from the macroscopic to the microscopic level at that time. Spectro-electrochemistry was established to gain mechanistic and dynamic information on electrochemical interfaces at the molecular level by developing *in situ* optical spectroscopic methods from the mid-1970s to early-1980s.[1] Raman spectroscopy was the first vibrational spectroscopy employed to characterize species on electrode surfaces as aqueous solution does not lead to notable interference to the surface signal. However, the Raman process has its intrinsic disadvantage owing to the very low detection sensitivity. Therefore, electrochemical Raman experiments without enhancement was impractical and just impossible for applications.

In order to overcome the fatal limitation in the detection sensitivity for surface species, Fleischmann, Hendra and McQuillan of University of Southampton devised a strategy to increase the number of adsorbed molecules and choose an adsorbate with a very large Raman cross section, such as pyridine (Py).[2] On the basis of their extensive experience in increasing the surface area of a Ag electrode by using an electrochemical roughening method, they applied about 450 potential oxidation and reduction cycles (ORC) to a Ag electrode in an aqueous electrolyte comprised of 0.1 mol L^{-1} KCl + 0.05 mol L^{-1} Py. The Raman spectrum obtained was of unexpectedly high quality and evidently due to the adsorbed Py in view of its electrode potential dependency.[2] All the major Raman bands changed markedly in intensity as the potential

State Key Laboratory of Physical Chemistry of Solid Surfaces and Department of Chemistry, College of Chemistry and Chemical Engineering, Xiamen University, Xiamen, 361005, China. E-mail: zqtian@xmu.edu.cn. E-mail: bren@xmu.edu.cn; Fax: +86-592-2085349; Tel: +86-592-2186979

De-Yin Wu is a full professor of Chemistry and a permanent research scientist in the State Key Laboratory of Physical Chemistry of Solid Surfaces. His interest is on the theories of SERS mechanisms, charge-transfer in electrochemical interfaces and molecular spectroscopy.

Jian-Feng Li obtained his BSc at Zhejiang University in 2003 and is now pursuing his PhD degree with Prof. Zhong-Qun Tian at Xiamen University. His thesis is concentrated on the synthesis of various types of core–shell nanoparticles that are used as non-traditional SERS substrates for detecting systems with very weak Raman signals.

Bin Ren is a full professor of Chemistry and a permanent research scientist in the State Key Laboratory of Physical Chemistry of Solid Surfaces. He won the Chinese Young Chemists Award in 2004 and the Chinese Young Electrochemists Award in 2007. His research interest is on TERS, in situ *electrochemical SERS and spectro- and interfacial-electrochemistry.*

Zhong-Qun Tian is a full professor at Xiamen University and serves as a director of State Key Laboratory of Physical Chemistry of Solid Surfaces. He is a Member of Chinese Academy of Sciences and Fellow of the Royal Society of Chemistry and member of advisory board of seven international journals. His main research interests are surface-enhanced Raman spectroscopy, spectro-electrochemistry and nano-electrochemistry.

was changed. They initially thought that it was the significantly increased surface area of the electrode that led to the intense surface Raman signals of Py. In retrospect, this was, in fact, the first SERS measurement and that roughened electrode was the first nanostructure exhibiting the SERS activity, although it was not recognized as such in 1974.

Jeanmaire and Van Duyne of Northwestern University soon tested the hypothesis that such a surface roughening leads to an increased surface area.[3] Further, they surprisingly found that, starting from the degree of the roughness used by Fleischmann *et al.*,[2] surface Raman signals increased as the surface roughness decreased. This was, in fact, the first demonstration that the SERS activity depends on the size of nanostructures. Subsequently, they carefully devised a procedure to measure the surface enhancement factor, wherein the signal intensity of a specific molecule on the surface is compared to that of the same molecule in solution; they discovered the 10^5–10^6 enhancement factor associated with SERS. After a protracted review process, presumably due to the reluctance of reviewers to believe an unorthodox concept of surface enhancement, their paper was eventually published in 1977.[3] Independently Albrecht and Creighton of University of Kent reported a similar result in the same year.[4] These two groups provided strong evidences to demonstrate that the enormously strong surface Raman signal must be caused by a true enhancement of the Raman scattering efficiency itself. The effect was later named surface-enhanced Raman scattering (SERS).[5] This landmark breakthrough opens up a great opportunity to design highly sensitive surface diagnostic techniques applicable to not only electrochemical but also biological and other ambient interfaces.

In the mid-1990s an important progress in electrochemical surface-enhanced Raman spectroscopy (EC-SERS) was made by which substantial surface Raman enhancements could be imparted to the VIIIB transition metals of importance for electrochemistry and catalysis. Our group developed several surface roughening procedures and demonstrated that SERS can be directly generated on pure Pt, Ru, Rh, Pd, Fe, Co and Ni electrodes, and their surface enhancements range in general from one to three orders of magnitude.[6] Since the early-2000s, the approach of replacing randomly roughened surfaces with well-controlled nanostructures of both coinage (*e.g.*, Au, Ag and Cu) and transition metals has been introduced as a very promising class of highly SERS-active substrate.[7] Up to now, molecular-level investigations by Raman spectroscopy on diverse adsorbates at various material electrodes have been realized. These advances have made Raman spectroscopy widely used in electrochemistry. Moreover, a systematic study on EC-SERS processes could be helpful for elucidating comprehensively SERS mechanisms.

In the following sections, we will first briefly survey important features of EC-SERS, followed by a brief outline of the EC-SERS experimental setup and procedures. The preparation of highly SERS-active nanostructured electrodes will be introduced. The methodology of Raman spectroscopy in the study of a variety of electrode surfaces will be discussed. This will be followed by a detailed description of electrochemical applications of SERS and analysis of EC-SERS spectra on the basis of the chemical and electromagnetic enhancement mechanisms. Finally, the prospect and further developments of this field are given with emphasis on emerging methodologies.

2 Features of electrochemical surface-enhanced Raman spectroscopy

The electrochemical surface-enhanced Raman scattering (EC-SERS) system generally consists of nanostructured electrodes and electrolyte. Thereby, an electrochemical double layer is formed in between, as the most important and complicated interfacial region. Like other branches of SERS, the basic research of EC-SERS can be sketchily divided into two trends: characterization and identification. For the identification purpose, the study is performed to demonstrate whether SERS is able to detect target species in terms of sensitivity and selectivity. For the characterization purpose, one should have a more comprehensive understanding of SERS including the enhancement mechanism and the surface selection rule, thus to evaluate the relative contribution of enhancement mechanisms to the total enhancement. Beyond the analytical aspect, EC-SERS has paid more attention to the characterization on the physical aspect and also made great efforts to provide really meaningful information for revealing the adsorption configuration or the reaction mechanism for electrochemistry.[8–11]

Generally, it has been widely accepted that the SERS enhancement effect is contributed by the electromagnetic field enhancement (EM) and chemical enhancement (CE).[12–14] The former is the main contribution to SERS signals in most SERS systems. While in electrochemical systems the latter also plays an important role especially in characterization of chemical species as it is closely associated with the chemical property of surface species and substrate. For a clear description of the contribution of both EM and CE mechanisms, the SERS intensity can be approximately expressed as[9,15,16]

$$I_{\mathrm{SERS}} \propto G_{\mathrm{EM}} \sum_{\rho,\sigma} |(\alpha_{\rho\sigma})_{\mathrm{nm}}|^2 \qquad (1)$$

where G_{EM} is the enhancement factor from the EM fields of the incident light and the scattered light on the surface. On the basis of the Maxwell equation, the EM enhancement is determined by the interaction of (incident and scattered) light and substrate, which depends critically on the excitation wavelength, the optical property of substrate and the surface morphology. From these different aspects, the EM enhancement includes several processes, such as the surface plasmon resonance, lightning-rod effect and coupling effect of the particle aggregate. These effects result in a giant SERS enhancement enabling the single-molecule detection.

The sum term of $(\alpha_{\rho\sigma})_{\mathrm{nm}}$ is the frequency-dependent polarizability, which is the molecular specific part resulting in the chemical enhancement. It describes the optical response of the molecular electronic structure and the interaction between the molecule and the metal surface. The chemical enhancement is contributed from the chemisorption interaction, the photon-driven charge transfer (CT) between adsorbate and substrate, and the coupling effect between the electron–hole pair and adsorbed molecules. Although these processes result in the

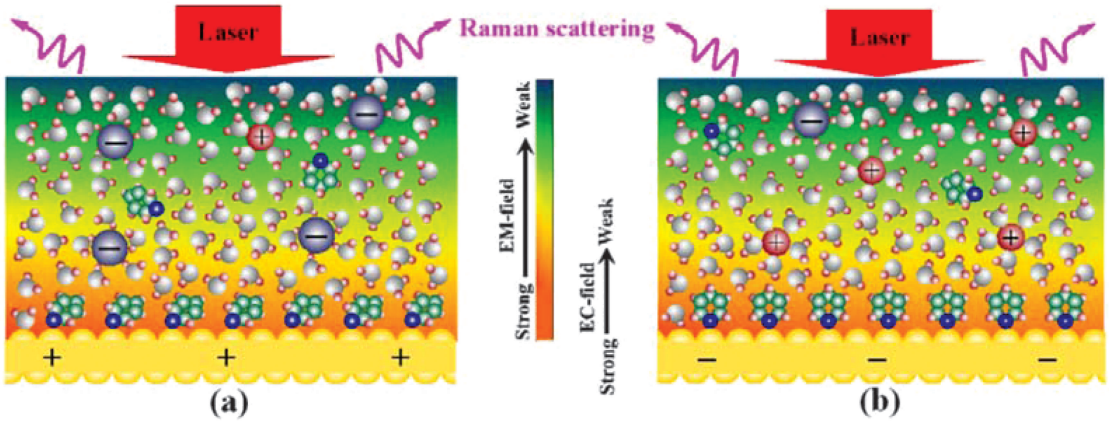

Fig. 1 Schematic diagrams of the electrochemical interfaces exhibiting SERS and with the coexistence of electromagnetic field and the electric field at the electrode potentials positive (a) or negative (b) to the potential of zero charge.

relative weak enhancement, they determine the frequency shift and relative intensity of the spectral bands, which is essential for the EC-SERS characterization.

Both chemical and physical enhancements can be influenced to some extent by changing the applied electrode potential, *i.e.*, the Fermi level of metal and dielectric constant of interfacial electrolyte, in an EC-SERS system. The former in particular can be strongly tuned by the potential, leading to drastic change of interfacial structure and property. This makes EC-SERS as one of the most complicated systems in SERS. In the following part, we will briefly introduce the features of EC-SERS, so that one may be able to fully harness the advantage of EC-SERS.

2.1 Electrochemical double layer of EC-SERS systems

As shown in Fig. 1, when a light illuminates a nanostructured electrode surface to excite a SERS process, a strong optical electric field is established in the electrochemical double layer region. As a consequence, there are two kinds of electric fields with distinctively different properties, the alternating EM-field and static electrochemical field (EC-field), co-existing in the electrochemical system. The EC-field could be quite strong as the potential drop occurs mainly over the compact layer with *ca.* one nanometer thickness or less and the diffuse layer.[17] It influences effectively the interaction (or bonding) between metal and the adsorbate, the surface orientation of the adsorbate and the structure of the double layer, which may in turn cause the redistribution of the surface localized optical electric field.

By adjusting the electrode potential, the density and polarity of the surface charge will change. When the electrode potential is more positive than the potential of zero charge (PZC), the surface will be positively charged and the water molecules interact with the surface *via* the negatively charged O end (see Fig. 1(a)). Meanwhile, other anionic species in the electrolyte may also approach the surface and molecules of interest may interact with the electrode surface. Taking the Py molecule for example, it can repel the surface water and interact with the surface *via* both the π orbital and lone pair orbital of N atom in a tilted configuration.[15,18] When the electrode potential is moved to negative of the PZC (Fig. 1(b)), the interaction of the electrode with the O end of water becomes weaker and that with the H end becomes stronger. Meanwhile, other cations are adjacent to the surface. Under this condition, Py may interact with the surface *via* the lone pair orbital of N atom, resulting in a vertical configuration. With the further negative movement of the electrode potential, the interaction is weakened further and changes from chemisorbed to physisorbed type or the Py molecule will even be desorbed from the surface.

2.2 Potential dependent SERS spectral characters

Another important and common feature of EC-SERS is that the SERS intensity strongly depends on the electrode potential. The change of the electrode potential may result in the change of the coverage and/or the adsorption orientation of the molecule, both of which will lead to a change in the SERS intensity.[6,15] It is also possible that even when the coverage or orientation does not change, the SERS intensity still change with the potential. The following two factors may mainly account for this phenomenon: the change of the bonding interaction of the molecule with the surface and/or the photon-driven CT mechanism. A change in bonding strength may affect the geometric and electronic structure of the molecule, which eventually leads to the spectral feature change of the molecule. In the case of photon-driven CT effect, one may expect two charge-transfer directions: metal to molecule and molecule to metal, which depend on the electronic structure of the adsorbed molecules and the electrode materials as well as the excitation wavelength.

This feature was first observed by Jeanmaire and Van Duyne in 1977. They demonstrated that the Raman intensities of the adsorbed Py is a function of the electrode potential with a laser excitation wavelength of 514.5 nm, as shown in Fig. 2.[3] According to the location of the intensity maxima in the potential-intensity profiles, the SERS bands can be divided into two groups. The first group shows intensity maxima at more positive potentials and could be detected in the whole potential region investigated. The bands at 1006, 1035 and 3056 cm^{-1} belong to this group. The second group includes the bands at 623, 1215 and 1594 cm^{-1}, whose intensities grow from very weak features at 0.0 V into strong intensity maxima at −0.8 V, and usually appear as new bands in the Raman

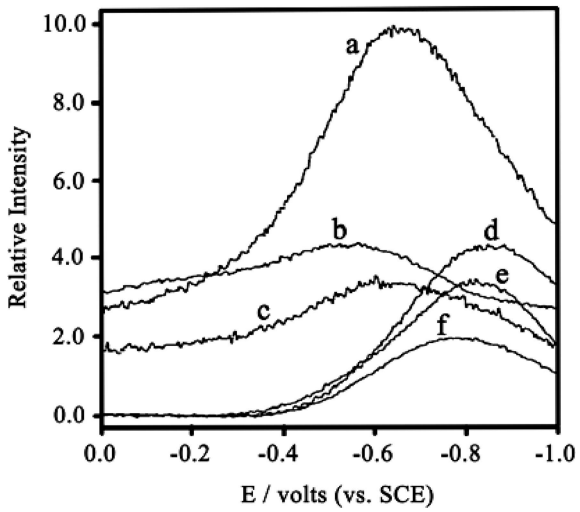

Fig. 2 The SERS intensity of the adsorbed pyridine on silver as a function of the electrode potential: (a) 1006 cm^{-1}, (b) 1035 cm^{-1}, (c) 3056 cm^{-1}, (d) 1215 cm^{-1}, (e) 1594 cm^{-1}, (f) 623 cm^{-1}. Laser excitation wavelength was 514.5 nm. The electrode potential was scanned at a rate of about 1 V s^{-1} beginning at 0.0 V *vs.* SCE. Each curve was a signal averaged over ten potential scans. (Reprinted with permission from ref. 3. Copyright 1977, Elsevier).

spectrum. The potential dependence of the Raman signal was thought to be from a composite effect of the surface coverage change of the adsorbate and the double layer electric field enhancement.[3]

Later, Birke and Lombardi *et al.* performed a systematic study on this interesting phenomenon and noted that the potential might tune the SERS intensity through the resonance-Raman polarizability term of the molecule–metal system.[15] Recently, based on density functional theory (DFT) calculations, Wu *et al.* and Zhao *et al.* investigated these vibrational modes of Py adsorbed on metals and showed that these modes have different responses to the bonding interaction and the CT mechanism.[19,20] The results indicate that both effects should be simultaneously considered for interpreting the complex potential dependence.

2.3 Electrode materials and excitation energy dependency

It is well known that the optical property of a material is closely associated with its electronic structure. The coinage metals as the most SERS-active substrates, having the prominent optical property of free electron metals, support the effective surface plasmon resonance (SPR).[21] However, the SPR effect is severely quenched for Cu and Au due to the d–sp electronic interband transitions when the excitation energies are higher than 2.2 eV. By contrast, the interband transition of silver occurs at an energy higher than 3.8 eV, corresponding to a wavelength shorter than 326 nm.

In comparison with the coinage metals, transition metals (VIII B element group) of practical importance in electrochemistry have very different electronic band structures, where the Fermi level is located at the d band and the interband excitation occurs in the whole visible light region. The interband electronic transition depresses the SPR quality of transition metals considerably.[6,22] Therefore, it reduces the effectiveness of SPR to show intense SERS, as observed in many experiments with visible excitation. It is of interest that the SERS excited by ultraviolet light (UV-SERS) has been observed unambiguously only from some transition metals so far, *e.g.*, Rh, Pd, Co and Ni, but not from the typical SERS-active substrates of coinage metals.[23]

Owing to the strong chemisorption interaction, the Raman scattering intensities of the vibrational modes of the adsorbate can be enhanced under certain condition. It should be noted that the binding interaction of the same kind of molecules was generally stronger on transition metal surfaces than that on coinage metals. When a strong chemical bond is formed, it will not only change the electronic structure of the adsorbate itself, but also influence to some extent the surface electronic structure. This may cause a shift of the SPR frequency and lead to a change of the local optical electric field at the metal surface.[24] Moreover, the change in the electronic distribution of the adsorbed molecule even at its electronic ground state may cause different enhancements for different vibrational modes.[19]

2.4 Electrolyte solutions and solvent dependency

When the electrolyte is changed, it will not only change the double layer structure of the electrochemical interface, but also influence the electrochemical reaction rates and even the reaction window. For example, the double layer will be compressed or expanded with the increase or decrease of the concentration of the electrolyte, respectively. Depending on the electrolyte, non-specific or specific adsorption may occur on the electrode surface. The specific adsorbed ions, due to the strong interaction with the metal surface, will possibly induce a shift of SPR bands. The electrolyte ion may also be coadsorbed with the adsorbates in a competitive or induced way. For example, thiourea may be coadsorbed with ClO_4^- and/or SO_4^{2-} on the Ag electrode.[11]

A change of the solvent will change the optical property of the electrochemical system. When organic solvents or ionic liquids are used, the electrochemical window will be drastically expanded and a marked change of the surface physical and chemical properties may be expected.[11,25,26] They not only change the oxidation potential of the metal electrode, but also eliminate the hydrogen evolution of water. When the solvent is changed from water to organic or ionic liquid solvents, the SPR frequency of the metal nanostructures will be red-shifted due to the increase in the refractive index of the host solvent.

2.5 The electrochemically influenced SERS enhancement

As mentioned above, the SERS effect in electrochemical systems is still contributed by the EM and CE enhancements, but it may be modulated by factors driven by the applied potential. The surface charge density of metal electrodes can be tuned by changing the applied potential with respect to the PZC, resulting in a shift in the SPR frequency.[25] Applying a positive potential to the electrode surface will lead to a damping and a redshift of the plasmon resonance band. On the contrary, a negative potential will result in an increase and blueshift of the plasmon resonance band. This phenomenon

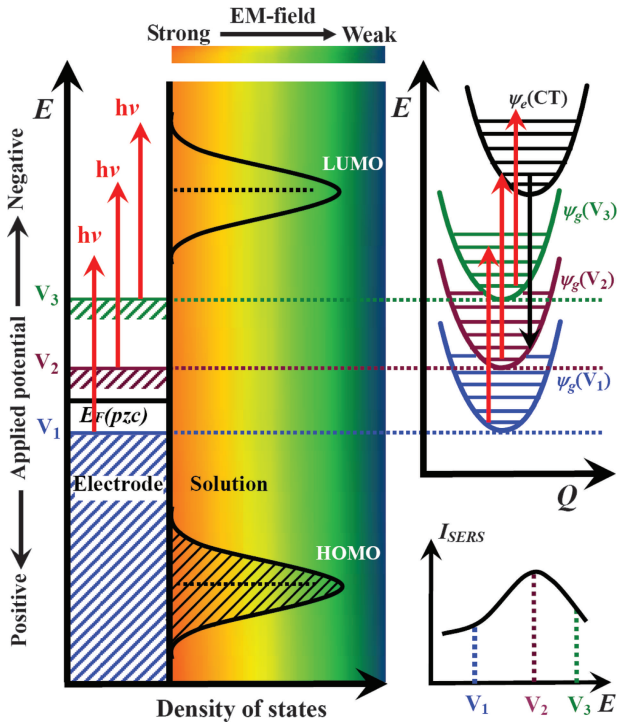

Fig. 3 Schematic diagrams of the photon-driven charge transfer from a metal electrode to an adsorbed molecule in the EC-SERS system. Left: the conceptual model of the energy levels changed with the electrode potential in the CT process. Right: the relevant energy states involved in the electronic levels and the vibrational levels in the CT process. Right bottom: the corresponding SERS intensity-potential profile. V_i denotes the applied potential.

can be explained by the charge density dependent plasmon frequency:[25]

$$\omega_p = 4\pi ne^2/m\varepsilon_0 \qquad (2)$$

where e and m are the charge and mass of an electron, n is the number density of free electrons, and ε_0 is the permittivity of vacuum. It is clear that an increase or decrease of n will result in a shift of the plasmon frequency. Meanwhile, the excess electrons in the conductance band will be easier to be polarized and have a large polarizability, in analogy to the lighting-rod effect of the electric field at a sharp surface protrusion, leading to a large enhancement effect at the negative potential.[27,28] According to the surface selection rule,[14,15] the physical effect will not change the relative Raman intensity of the vibrational modes with a same irreducible representation, while the chemical effect will.

The potential and metal dependent SERS intensity observed in many EC-SERS systems gives strong evidences that the chemical enhancement is cooperative with the EM enhancement, as illustrated in Fig. 3, where HOMO and LUMO denote the highest occupied molecular orbital and the lowest unoccupied molecular orbital of the adsorbed molecule, respectively. $\psi_g(V_i)$ and $\psi_{CT}(V_i)$ denote the molecular adsorption ground state and the photon-driven CT excited state formed from a filled level of the metal to the LUMO of the adsorbed molecule at an applied potential, V_i. The energy position of the CT state is assumed to be independent of the potential. The SERS signal first increases and then decreases with the negative movement of the electrode potential. This change of SERS intensity could be explained through the photon-driven CT from metal to molecule using the concept of energy level or energy states. As can be seen on the left side of the figure (energy level concept), at an applied potential of V_1, it is insufficient to produce the photon-driven CT states on the surface with an excitation energy of $h\nu$. As a result, the change of the relative SERS intensity could be determined mainly by the bonding effect.[19,20] When the potential is changed to V_2, due to the increase of the Fermi level of the metal electrode, the excitation energy matches the required CT energy, leading to a resonance-like Raman scattering and a significant enhancement in the SERS intensity of the relevant vibrational modes. However, if the potential is further negatively shifted to V_3, the excitation energy does not fall in an ideal resonance condition. Therefore, the contribution of CT states to the SERS signal will decrease.

The right part of Fig. 3 presents a conceptual picture relevant to not only the energy level but also the energy states with the vibrational coordinates. It displays much clearly the change of the surface vibrational energy of the adsorbate with the electrode potential. It should be noted that each energy level represents the total energy of the combined system of the adsorbed molecule and interacting metal electrode (molecule/metal) in the excited or ground electronic state that can be influenced by the potential change.

The photon-driven CT enhancement is considered a resonant Raman-like enhancement,[15,29,30] which is associated with the excited state of molecule/metal system and the charge transfer between the molecule and the metal surface (or adatom and adclusters). Otto *et al.* considered that the CT process proceeds with a four-step process, the generation of the surface plasmon excitation, the formation of the negative ionic molecule, electron returns to metals and finally the emission by the radiating photons.[29] Alternatively, Birke and Lombardi adopted a two-state Franck–Condon or three-state vibronic processes to predict the potential dependence of the SERS intensity.[15]

From the above, one may conclude that EC-SERS is among the most complicated SERS systems. On the other hand, it gives more flexibility to investigate the interfacial structure and mechanism of complex systems by changing the experimental conditions, such as the electrode material, electrolyte, solvent, electrode potential and temperature in both fields of SERS and electrochemistry.

3 Experimental techniques of EC-SERS

In a typical EC-SERS study, the electrochemical system is investigated while the electrode potential is changed and the spectral response (including the intensity and frequency change or even the appearance of new bands) is recorded. In most cases, the experimental data will be interpreted by analyzing the intensity or frequency change of some characteristic bands (vibrational modes), which may directly reflect a change in the surface coverage, orientation, structure, composition and morphology, and sometimes may indicate the involvement of a certain kind of surface enhancement

mechanism. Therefore, it is very essential to calibrate both the collection efficiency and frequency accuracy.

Since microprobe Raman instruments are now the prevailing instrument in the market, it has become a common practice to use the very sharp and intense peak of 520.6 cm^{-1} of a single-crystal Si wafer (preferably Si(111)) to calibrate both the frequency and sensitivity. However, if the excitation line shifts to the UV region, it is better to use the 1333.2 cm^{-1} band of diamond as a calibration standard. In some old or simple Raman systems, the frequency linearity or accuracy may not be very good and it will be helpful to choose a standard close to the investigated frequency region. For example, 219.1 cm^{-1} of sulfur, 801.3 cm^{-1} of cyclohexane, 2229.4 and 3072.3 cm^{-1} of benzonitrile can all be used as the frequency standard.[31] It is quite common that the collection efficiency of Raman systems will change from day to day. Therefore, in order to compare the intensity of Raman spectra collected on different days, it is better to normalize the intensity with the intensity of the 520.6 cm^{-1} peak of a Si wafer.

Before a new EC-SERS study, it is important to first obtain the normal Raman spectrum of the species in its original form, such as the pure liquid, solid, or even some standard samples of the expected products, and the Raman spectrum of the solution to be used in the EC-SERS. When the concentration is too low, one may consider increasing the concentration to improve the quality of the spectrum. Then, these good-quality spectra will serve as the references for interpreting the EC-SERS result. If the spectrum is too complex to make the assignment, an isotopic substitution of specific atoms or theoretical calculations of normal modes may be helpful. Before the EC-SERS study, it is very helpful to measure the electrochemical cyclic voltammogram to obtain the characteristic potential for the *in situ* EC-SERS study.

3.1 Experimental set-up

Fig. 4 displays the experimental setup for *in situ* EC-SERS. It includes a laser to excite the SERS of samples, a Raman spectrometer to disperse and detect the Raman signal, a computer to control the Raman instrument for data acquisition and manipulation, a potentiostat or galvanostat to control the potential of the working electrode and an EC-SERS cell to accommodate the reaction. It may be necessary to place a plasma line filter in the incident path for some lasers to obtain a truly monochromatic incident light. The detector of the Raman system can be single channel (PMT, photomultiplier tube or APD, Avalanche photodiode) or multi channel (CCD, charge coupled device). The latter is now becoming a dominant configuration. In the case of time-resolved study, it may be necessary to have a wave function generator to generate various kinds of potential/current controls over the electrode and to trigger the detector accordingly to acquire the time-resolved SERS signal.

3.2 EC-SERS cell design

The EC-SERS cell is the core component of the EC-SERS experimental setup. It is relatively simple and more flexible in the design for aqueous electrolytes. A typical cell configuration used in our lab is shown in the left-bottom corner of Fig. 4. It consists of a conductive SERS-active working electrode, an inert counter electrode (usually Pt wire ring) to form a closed circuit and a reference electrode (usually saturated calomel electrode, SCE, or a Ag/AgCl electrode) to indicate the potential of the working electrode. The three electrodes should be assembled in a good relative geometric position to allow both efficient Raman and accurate electrochemical measurements. For example, the reference electrode should be placed in a compartment with a Luggin capillary tip placed very close to the working electrode to ensure an accurate control of the potential. An optically transparent quartz or glass window may be used to protect the solution or electrode from being contaminated and interfered by the ambient atmosphere. For non-aqueous systems, one has to be extremely cautious about the absorption of water or exchange of gas with the environment, which may severely alter the reaction mechanism of the non-aqueous systems. Thus, the cell for non-aqueous systems should be water- and gas-tight, realized with an O-ring design. The reference electrode should be water free and the readers may refer to ref. 32 for selection of proper type of reference electrodes or simply use a metal wire as a quasi reference electrode.

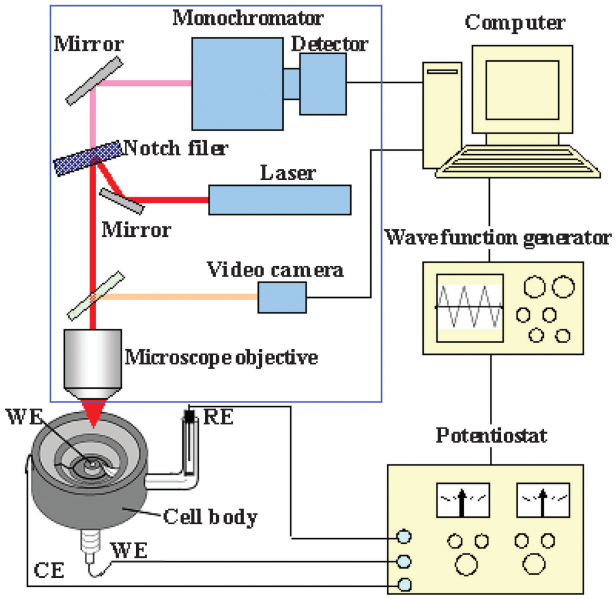

Fig. 4 Diagram showing the experimental setup for EC-SERS, which includes a Raman spectrometer (in the blue block), potentiostat, computer, wave function generator and an EC-SERS cell. WE: working electrode, CE: counter electrode, RE: reference electrode.

3.3 Improving the detection sensitivity

Detection sensitivity has always been a key concern to optical methods for probing electrode surfaces because normally only monolayer or even sub-monolayer species (*ca.* 10^{15} per cm^2) are presented, especially for a weak Raman scatterer. Thus, how to increase the detection sensitivity of EC-SERS becomes a very important issue to the application of Raman spectroscopy in electrochemistry. There are several possible ways to

improve the detection sensitivity: (1) to use a high numerical aperture microscope objective with a long working distance to increase the collection efficiency; (2) to increase the laser power as far as possible below the damage threshold since the Raman signal is linear to the laser power; (3) to use the potential difference method to extract the very weak interfacial signal from the bulk signal; and (4) to select a suitable wavelength to utilize the resonant Raman effect. By properly treating the electrode surface, one may be able to obtain very strong SERS from Ag, Au and Cu surfaces and mild SERS signals from Pt, Rh, Ni, Co and Fe surfaces.

3.4 Preparation of SERS-active electrode surfaces

It is well-known from previous SERS studies of Au, Ag and Cu that a necessary, but not sufficient, requirement for a large surface enhancement is some form of surface roughness. With the development of nanoscience and nanotechnology, the substrates that can be used for SERS have also been expanded from massive metal electrodes and metal colloidal sols, to template fabricated substrates and nanoparticle assembled electrodes for larger enhancement. We will introduce in this section several methods to fabricate SERS-active substrates suitable for EC-SERS. For other types of substrates, the readers may refer to our previous review chapter.[33] No matter which kind of electrodes we are using, special attention has to be paid to remove impurities from the surface to eliminate any possible artifact that may interfere with the measurement. In practice, there are several ways to realize this goal, including electrochemical cleaning by potential cycling, hydrogen evolution, or use of other strong adsorbates followed by desorption or electrochemical oxidation.

Electrochemical oxidation and reduction cycle(s) (ORC)

Generally the electrodes for the EC-SERS study are made by sealing a metal rod into an inert Teflon sheath. To improve the reproducibility of the experiment, the electrode surface should be first mechanically polished with alumina powders down to 0.3 μm, rinsed with ultra pure water, and sonicated to remove any adhering alumina. One may also use severe hydrogen evolution or electrochemical cleaning to remove surface impurities. Then, the electrode can be activated by electrochemical oxidation and reduction cycles. Depending on the metal entity, different ORC conditions will be used. The experimental variables in the ORC include the oxidation and reduction potentials, the type of potential–time function (triangular-wave potential sweep or double potential steps), and the amount of charge passed during the oxidation step. The applied potential, especially the oxidation potential, is dictated by the electrolyte and the electrode used. Here we only describe the method for Ag, Au and Pd; for readers who are interested in other metals, please refer to ref. 33. All the potentials mentioned below are referred to an SCE reference electrode.

Ag electrode. A mechanically polished mirror-finish silver electrode was immersed in 0.1 mol L^{-1} KCl solution with its potential kept at −0.25 V for a while to reduce the surface oxide. Then the potential is pulsed to +0.18 V for 8 s for oxidation. After that, the potential is moved negatively to keep the reduction current density at 3 mA cm^{-2} until a complete reduction of the dissolved silver and the formed silver chlorides. Finally the potential was moved back to −0.25 V for complete reduction and the electrode is light gray to light yellow. To obtain a Ag substrate free of chloride, the electrode should be held at −0.60 V in 1 mol L^{-1} $NaClO_4$ solution. Afterwards, the potential is stepped from −0.60 to +0.55 V for oxidation for 3–5 s. Then, the potential is switched back to −0.10 V for complete reduction. The color of the electrode will be dark green to dark brown.

Au electrode. To obtain a SERS-active Au substrate, one may follow the ORC procedure given by Weaver and co-workers.[34] The Au electrode is first electrochemically cleaned in 0.1 mol L^{-1} H_2SO_4 solution in the potential range of −0.25 and 1.5 V. After rinsing with ultrapure water, the Au electrode is kept at −0.3 V in 0.1 mol L^{-1} KCl until the stabilization of the current. Then, the potential is scanned to 1.2 V at 1 V s^{-1}, set for 1.2 s for oxidation, then scanned back to −0.3 V at 0.5 V s^{-1} and set for 30 s for reduction. The cycle is repeated for about 15 min and the final potential should be −0.3 V to ensure a reduced state of the electrode. This roughening process results in an Au surface with a brown appearance.

Pd electrode[35]. The above potential cycling or step method used for Ag and Au electrodes can also be employed to roughen other relative active metals, such as Fe, Co, Ni, Cu. These methods are essentially based on the dissolution and re-deposition of the surface atoms. However, they do not work well on some Pt-group metals, such as Pt, Rh, Pd, which are very stable and can easily form a compact oxide layer to prevent further oxidation of the surface. We have developed a repetitive roughening method for Pd, which resulted in a reasonable SERS activity. The basic principle is to form a thick Pd oxide layer on the surface as a result of the exchange of the surface oxygen with the bulk metal atoms, leading to further oxidation of the inner layers of the surface by applying a repetitive periodic potential to the Pd electrode. Then, the surface oxide is reduced at a suitable potential to form a metallic surface. The wave form used for the Pd electrode is $E_{low} = -0.40$ V, $E_{high} = +1.7$ V, $f = 600$ Hz and the final reduction potential is −0.1 V for Pd. The solution is 1 mol L^{-1} H_2SO_4. The surface roughness can be controlled by the roughening time from a few seconds to several minutes depending on the purpose of the study. The SEM image of the roughened Pd electrode is given in Fig. 5(a) and consists of nanoparticles with a size around 50 nm. Readers may refer to other papers for roughening methods for Pt and Rh.[33]

Preparation of SERS substrates using metal nanoparticles

The electrochemical roughened SERS substrates have a rather broad distribution of roughness, as can be seen in Fig. 5(a). This ill-defined geometry is unfavorable for understanding the interfacial structure and maximizing the SERS activity. Alternatively, with the nanotechnology, it is now possible to synthesize or fabricate metal nanostructures of various shape and size with a narrow size distribution. The nanoparticles assembled on an electric conductive substrate can significantly improve the surface uniformity of the EC-SERS substrate.

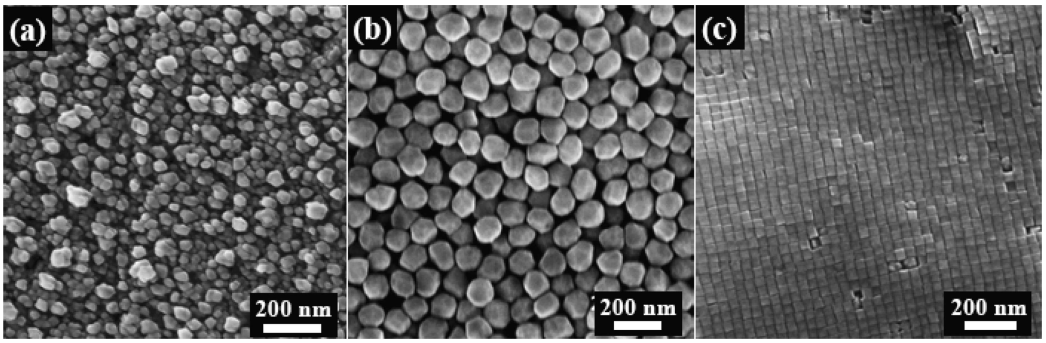

Fig. 5 SEM images of three typical SERS-active electrodes for EC-SERS: (a) an electrochemically roughened Pd electrode, (b) Au nanoparticle assembled film electrode and (c) Au-core–Pd-shell (Au@Pd) nanocube assembled film electrode.

Therefore, use of nanoparticle sols or assembled nanoparticles as SERS substrates has been booming in recent years.

Here we only briefly introduce the synthesis methods for some nanoparticles most frequently used in our lab. Au nanospheres can be prepared using the seed mediated growing method starting from 12 nm Au nanospheres using Frens' method,[36] and nanospheres with a diameter size ranging from about 12 to 200 nm with very uniform distribution can be routinely obtained, with the 130 nm nanospheres showing the strongest SERS with 632.8 nm excitation. Au nanocubes can also be prepared by the seed mediated method, however, only in the presence of a capping agent such as CTAB. By controlling the concentration of the seeds, Au nanocubes of different sizes can be obtained, with the 83 nm cubes showing the strongest SERS with 632.8 nm excitation.

Normally transition metal nanoparticles show relative weak SERS activity in comparison with Ag and Au nanoparticles. In order to improve the SERS activity, one may utilize the borrowing SERS strategy by coating a thin layer of transition metal over Au nanoparticles.[7,10] For example, when different amounts of H_2PdCl_4 are added into a sol solution containing Au nanocubes of desired size, Au core Pd shell (Au@Pd) nanocubes with controllable shell thickness (*ca.* 2–10 atomic layers) can be obtained. Boosted by the long-range effect of the enhanced EM field generated by the highly SERS-active Au core, the originally low surface enhancement of the transition metal can be substantially improved giving total enhancement factors up to 10^4–10^5. Readers may refer to refs. 7 and 37 for the synthesis of other kinds of nanoparticles.

The synthesized nanoparticles will then be dispersed over a conductive solid electrode surface, such as glassy carbon, indium tin oxide (ITO), Au, Pt, or Pd surface, and used for EC-SERS. To prepare the substrate, a solid electrode should be thoroughly polished or cleaned before assembly. Then a drop of sol solution containing nanoparticles are dispersed on the electrode surface and left to dry in air or assisted by a vacuum pump. Fig. 5(b) shows the typical morphology of a substrate assembled with Au nanospheres and Fig. 5(c) the Au@Pd nanocubes.

It is obvious that the nanoparticle assembled films show significantly improved surface uniformity in a large area compared with the electrochemically roughened substrate as shown in Fig. 5(a). The surface signal difference over the whole surface is less than 10%. Alternatively, the nanoparticles can also be assembled on the substrate *via* bifunctional molecules, such as (3-aminopropyl)trimethoxysilane (APTMS) or thiols, to form a SERS-active substrate. The use of such nanoparticle assembled film electrode is increasing in recent years in EC-SERS studies due to a high SERS activity and high reproducibility.

Fabrication of ordered SERS substrate by template method

Although nanoparticle film electrodes show very good surface uniformity, it is difficult to control the spacing of the nanoparticles to optimize the SERS activity. Template methods are promising in obtaining very ordered substrates and controlling the inter-particle spacing. Among various ordered templates, nanosphere lithography (NSL) and anodic aluminium oxide films (AAO) have been most widely used for preparing SERS-active substrates.

AAO template method. When electrochemically polished aluminium foil is oxidized in phosphoric or oxalic acid solution, a very ordered two-dimensional array of cylindrical nanopores can be obtained. The diameter of the pores can be tuned from 15 to 150 nm by adjusting the anodic voltage, the solution pH and composition, and the temperature during the formation of the AAO film. Then by applying an alternating current with a frequency of *ca.* 50 Hz and a voltage (2 to 20 V depending on the thickness of the barrier layer of the AAO film) to the AAO film in the solution containing a desired metal salt followed by etching in the dilute phosphoric acid, a well-ordered and high SERS-active metal nanowire substrate can be obtained.[6] The main difficulty for such kinds of substrates for EC-SERS is how to conveniently obtain a satisfactory electric contact to the nanowires to allow potential control.

Nanosphere lithography. NSL has been well developed mostly through the work of the groups of Van Duyne[38] and Bartlett.[39] This most promising method can produce nanostructured substrates with a precise control over the shape, size and interparticle spacing, the detailed procedures are shown in Fig. 6.

The substrate for EC-SERS should be conductive, such as ITO or evaporated metal substrate over glass, which is thoroughly cleaned for assembly. Then, monodispersed polystyrene or SiO_2 nanospheres of the desired diameter are self-

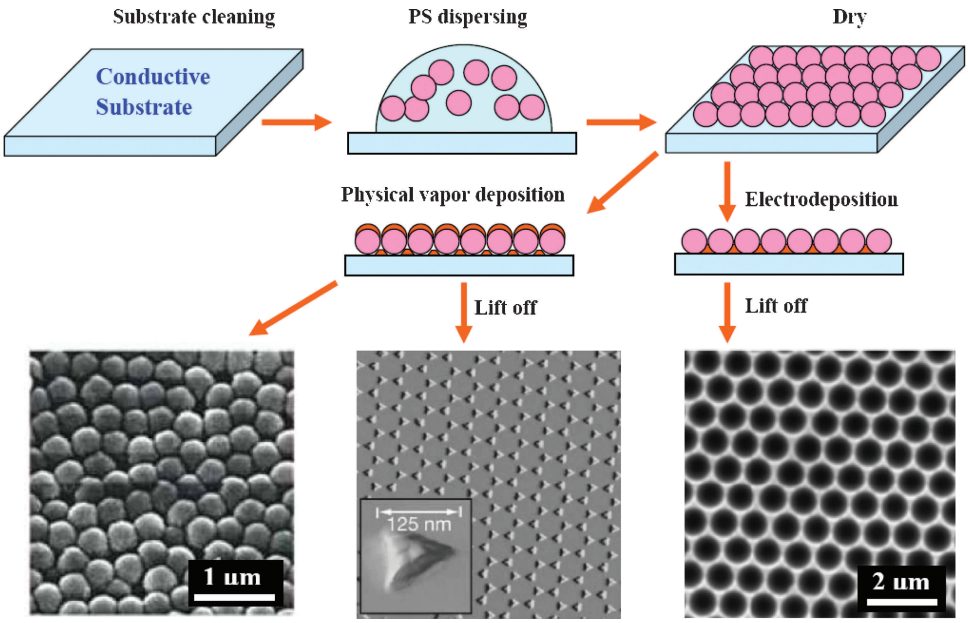

Fig. 6 Schematic diagram of template methods using nanosphere lithography to fabricate ordered nanostructured SERS-active substrates, redrawn according to the published works of Van Duyne's group (from ref. 38) and Bartlett's group (from ref. 39).

assembled on the substrate to form a very ordered single or multi-layer colloidal crystal template or mask for metal deposition. Afterwards, a metal layer is deposited by physical vapor deposition or electrochemical deposition on the substrate to a controlled thickness, which will then result in three types of structured SERS substrate: (a) physical vapor deposition on the nanosphere template leads to the formation of metal (*e.g.*, Ag) "film over nanosphere" (FON) surface; (b) the removal of nanospheres of the FON surface by sonicating the entire sample in a solvent results in surface confined nanoparticles with a triangular footprint; (c) electrochemical deposition followed by the removal of the sphere leaves a thin structured film containing a regular hexagonal array of uniform segment sphere voids. The surface morphologies of the three types of surfaces are shown in the lower panel of Fig. 6.

4 Applications of EC-SERS

Since the first SERS (also EC-SERS) report of Py adsorption on a roughened Ag surface, thousands of papers have been published on various aspects of SERS, including over 500 papers dealing with EC-SERS. Due to the page limit of this review, we are not able to cover all these works. Instead, we list in Table 1 the selected systems that have been investigated by EC-SERS. Most of this work deals with the adsorption and reaction of inorganic species, organic molecules and biomolecules in aqueous solutions. Only a few of them deal with non-aqueous systems and even ionic liquids. The excitation wavelength has also been expanded from the near-IR to the UV region in recent years.

For the EC-SERS application, a combined analysis of these spectral features from the experimental and theoretical aspects is essential, by which we are able to obtain the important information of chemical bonding, orientation and even electrochemical reaction of the molecules at the electrode surfaces, thereafter to understand the interfacial structure. As mentioned above, Py was the first molecule used in demonstrating the SERS effect and has been a very important probe molecule thereafter to test the SERS activity and surface properties of a new SERS substrate.[2–4,6] The relative intensities and frequency shifts of the major bands of Py are very sensitive to the electrode potential and the surface properties of the metal surfaces. These phenomena cannot be solely interpreted with the electromagnetic enhancement effect, and consideration from chemical effects needs to be taken into account. Only when we are able to adequately interpret the phenomena observed in this seemingly simple Py system, can we say that we understand EC-SERS and then provide the meaningful information for the characterization of surface chemistry so as to exert the full potential of SERS.

In the following, we limit ourselves to the discussion of three important systems in EC-SERS to illustrate how to perform systematic studies. First, SERS of Py on different metal surfaces will be discussed in detail for illustrating how EC-SERS can be used to characterize the surface adsorption and molecule–metal interaction. It also reveals how the frequencies and the intensities of SERS of Py are correlated to the chemical interaction between Py and the metal surface and the adsorption orientation. Then, we will briefly introduce one of the most important systems in electrochemistry, the structure of interfacial water. A satisfactory interpretation of this special system also needs a combined consideration of the EM and chemical enhancement mechanisms. Lastly, we will demonstrate how SERS can be used to monitor the dynamics of surface reactions by using time-resolved SERS.

4.1 Pyridine adsorption on different metal surfaces

For the EC-SERS characterization, the first step is to carefully assign the main vibrational modes of the molecule of interest.

Table 1 Partial list of SERS study related to electrochemistry

Adsorption	
Inorganic species	**SCN^-**: Ag, Au, Pt, Rh, Fe; **CN^-**: Ag, Au, Pt
	Cl^-, Br^-, I^-: Au, Ag, Pt; **H_2O**: Cu, Ag, Au, Pd, Pt, Rh, Ru
Organic molecules	**Pyridine**: all known SERS substrates
	Benzotriazole, **thiourea**: Ag, Cu, Fe, Ni, brass
	Benzene: Ag, Au, Pt, Pd, Rh, Ru
	Pyrazine: Au, Ag, Pt; **Imidazole**: Fe, Ni, Co, Ag
	Mercaptopyridine: Ag, Au; **Benzenethiol**: Ag, Au, Pt
	Conducting polymers: Au, Ag; polypyrrole, polyaniline, polythiophene, polyacetylene
	Dyes: Au, Ag: R6G, Crystal Violet, Methylene Blue
Biomolecules	**Ag**: Cyt c, enzymes porphyrin, hemoglobin, nicotinic acid, amino acids, DNA bases,
	Au: hemoglobin, dsDNA, ssDNA, oligonucleotide, Anti-IgG, bilayer lipid membrane, NADH
Reaction	
Electrocatalytic reactions	**Pt**: hydrogen, CO, CH_3OH, HCHO, HCOOH ethanol,
	Pd: CO, CH_3OH, hydrogen; Rh: CH_3OH, CO, hydrogen
	Ag: O_2, CO_2 reduction; **Cu**: CO_2 reduction
	Au: Acetylene, ethylene
Redox reactions	**Au, Ag (SAM modified)**: cytc, Heme, $Fe(CN)_6^{3-}$, Laccase
Time resolved-SERS (TR-SERS)	**Ag**: *p*-nitrobenzoic acid, 4-cyanopyridine, thiourea
	Au: 9,10-phenanthrenequinone
Electrodeposition	**Ag, Au**: thiourea, 4-cyanopyridine, cyanide, polyethylene glycol
Nonaqueous systems	
Organic solvent	**Pt**: CO, pyridine, CH_3CN, CH_3OH, HCOOH
	Ag: $Ru(bipy)_3^{2+}$/acetonitrile, H_2O
Ionic liquid	**Ag**: $BMIPF_6$
UV-SERS	
Adsorption	**Pt, Rh, Ru Pd, Co**: pyridine, SCN^-, CO, Adenine
Substrate	
Planar electrodes	Ag, Au, Cu, Pt, Rh, Pd, Fe, Co, Ni, Zn, Cd, Al
Nanoparticles	Ag, Au, Pt, Rh, Pd, Au@Pd,[a] Au@Pt, Au@Co, Au@Ni
Template substrate	**AAO**: Cu, Ag, Au, Pt, Ni
	PS: Ag, Au, Pd, Pt

[a] Au@Pd: Au core Pd shell nanoparticles, similar denotation for other core–shell nanoparticles.

The Py molecule has 11 atoms and C_{2v} symmetry point group. The molecular coordinates are defined as follows: the z axis is along the C_2 axis, the y axis along the molecular plane, and the x axis perpendicular to the molecular plane, resulting in $3n - 6 = 27$ fundamentals with four irreducible representations, $10a_1 + 3a_2 + 5b_1 + 9b_2$. Under the C_{2v} point group, all these modes are Raman active. However, in the normal Raman spectrum of pure liquid Py (Fig. 7(a)), only two bands at 990 and 1027 cm^{-1} can be clearly observed in the middle frequency region corresponding to the ring breathing mode (ν_1, Wilson notation) and symmetric triangular ring deformation (ν_{12}), respectively.[40] Other modes are too weak to be observed in the normal Raman spectrum. In the normal Raman spectrum of a Py aqueous solution, the ν_1 band blue shifts to 1002 cm^{-1}, indicating that this mode is sensitive to the chemical environment.

High quality SERS spectra (Fig. 7(a)) of Py can be easily recorded from coinage metal (silver, gold and copper) and transition metal (such as platinum) surfaces. For the convenience of comparison, Fig. 7(a) and (b) display the SERS spectra obtained on different metal surfaces under a similar electrochemical condition: peak potential or open circuit condition. Both the spectra of the pure liquid and the aqueous solution are given for comparison. At the open circuit potential, the frequency of the ν_1 mode blueshifts from 1002 cm^{-1} for the free Py in aqueous solutions to 1007 cm^{-1} for Ag, and to 1012, 1017 and 1018 cm^{-1} for Au, Cu and Pt electrodes, respectively. Meanwhile, the relative Raman intensity of the ν_{12} mode to the ν_1 mode significantly decreases after interacting with metal except for Ag. In Fig. 7(a), the peak at about 1600 cm^{-1} is weaker than the ν_1 peak on all four metal electrodes.

The potential dependent spectral character is the key issue to be investigated in detail. If we extract the spectrum at potentials with the maximum intensity (ν_1 mode) from the potential-sequence spectra, we obtain Fig. 7(b). By comparing Fig. 7(a) with Fig. 7(b), we find that the potential to obtain maximum intensity (peak potential) are all at the negative side of the open circuit potential and at least the following three

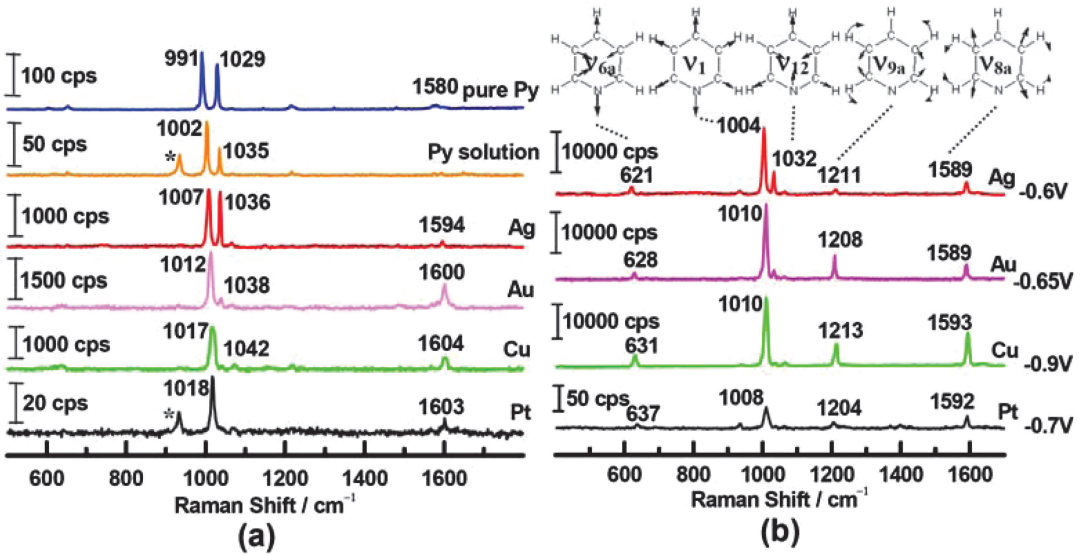

Fig. 7 Surface-enhanced Raman spectra of pyridine adsorbed on roughened Ag, Au, Cu and Pt electrodes at the open circuit potential (a) and at the peak potential (*vs.* SCE) of the ring breathing mode (b). The excitation line is 632.8 nm. For comparison Raman spectra of pure liquid pyridine and an aqueous solution (0.1 M $NaClO_4$ + 0.1 M Py) are also shown, the asterisked peak at 934 cm^{-1} is from ClO_4^-.

spectral changes can be extracted upon negative movement of the electrode potential. First, the peak frequencies redshift due to the change of the electrode potential. Second, the relative Raman intensities of the ν_{12} mode to the ν_1 mode decrease on Ag but remain almost unchanged on Au, Cu and Pt electrodes. Third, the three bands at 624, 1218 and 1598 cm^{-1} become stronger at the peak potential than that at the open circuit potential. Raman signals of other modes are still too weak to be observed over all the potential range investigated. On observing these features, it is natural to ask the reason for the frequency shift and the relative intensity change of Py upon interacting with the metal surface and the potential change.

To understand the observed phenomena, it is necessary to first analyze the binding interaction between Py and the metal electrodes, *i.e.*, the adsorption configuration. It is well known that the adsorption interaction depends on the property of the frontier molecular orbitals and the band structure of electrode materials. Fig. 8 shows five π-type molecular orbitals and the lone pair orbital of nitrogen of Py. For a free Py molecule approaching a metal surface, many possible configurations have been suggested on the basis of different experimental techniques.[41] However, taking into account the molecular structure of Py, the following three configurations are the most probable: (a) flat configuration with π-type bonding; (b) upright configuration with a σ bond through the lone-pair electron donation to the unoccupied orbital of metal atoms; and (c) a tilted configuration with a cooperative contribution from the σ and π interaction.

It has been found that the frequency of the ring breathing mode of aromatic rings decreases significantly at the flat configuration due to the interaction between the π-type orbitals and metal surfaces.[42] However, up to now, such a phenomenon has not been observed experimentally for Py in electrochemical systems. Even for Py adsorbed on the Pt electrode, the ring breathing frequency clearly blueshifts with respect to the 991 cm^{-1} of the pure liquid. Accordingly, it was suggested that Py should interact with the surface *via* the N-end in an upright or slightly tilted configuration when the surface coverage reaches a monolayer or the potential is negative or not too positive than the potential of zero charge.

When Py adopts an upright configuration on metal electrode surfaces, it binds to the electrode surface through the lone-pair electrons of nitrogen that interacts with the conductance band of the surface metal. Molecular orbital theory reveals that the strength of the binding interaction is determined by the match in symmetry and energy as well as the overlap of interacting orbitals. The DFT calculation based on the metal cluster model reveals that the binding interaction of Py with the IB metals Cu, Ag, Au weakens following the order of Cu ~ Au > Ag. Indeed, the adsorption interaction for Ag is very weak. This is due to a smaller d-to-s excitation energy of the Cu and Au cluster than the Ag clusters and therefore an easier hybridization of the s and d_{z^2} orbitals of Cu and Au.[18,40] Furthermore, we found that the binding interaction is sensitive to the binding orientation but is insensitive to the size of the metal cluster. This is because the most important unoccupied orbital in the energy and symmetric matching is similar in different metal clusters.[43] It should be noted that, however, the electron back-donation from the metal atoms to the π-type anti-bonding orbital is very weak in all these complexes. The binding interaction of transition metal clusters (such as Pt) is stronger than that of the coinage metals due to a lower unoccupied level and the participation of d orbitals in the bonding.

The frequency shift may be interpreted by the chemical binding interaction and the vibrational coupling when Py is adsorbed on the electrode surface. As seen in Fig. 8, the binding interaction is mainly due to the σ-type bonding between the lone pair orbital of the nitrogen atom and metals, and π-type bonding from the $2b_1$ orbital of Py and metals. The latter will significantly enhance the strength of the two parallel C–C bonds due to the decrease in the antibonding character,

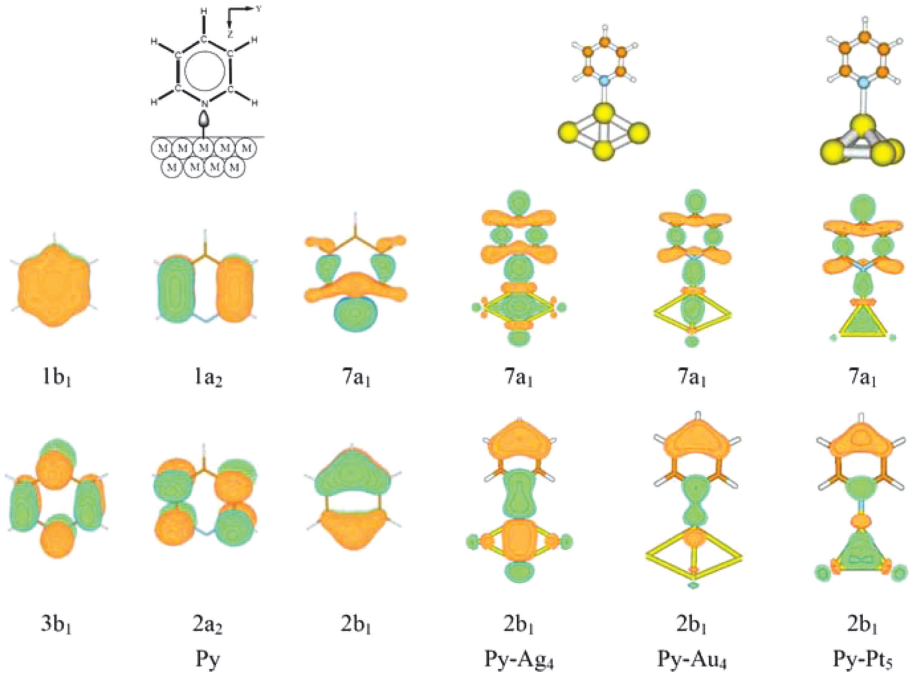

Fig. 8 Electron cloud densities of pyridine and pyridine interacting with Ag_4, Au_4 and Pt_5 clusters in an upright adsorption configuration: $7a_1$ denotes the lone pair orbital of nitrogen of pyridine.

resulting in a blueshift of frequencies of the ν_1 and ν_{8a} modes.[40] However, the chemical bonding cannot explain the frequency shift of the ring deformation modes of ν_{6a} and ν_{12} modes. Instead, the vibrational coupling may play an important role. For example, the ν_{6a} mode hardly couples to the other intramolecular vibrations but has a strong coupling with the Py–metal adsorption bond.[40] As a consequence, the frequency blueshift of the ν_{6a} mode will sensitively reflect the strength of the binding interaction between Py and metal electrodes.

From the above discussion, we see that the chemisorption of Py is through the donation interaction of the lone pair electrons of nitrogen and the short-range π bonding interaction with metal surfaces. In the electrochemical interface, the negatively moved potential will weaken the adsorption bond, resulting in the redshift in the vibrational frequencies of the a_1 modes.

It is interesting that according to selection rules of SERS based on the EM mechanism, the four intense SERS bands all belong to the totally symmetric modes (a_1) under a C_{2v} point group symmetry and therefore should be equally enhanced. However, the potential dependences of these four bands are distinctively different. The EM enhancement mechanism cannot account for the relative intensity change of these modes.[44] Therefore, the CE effect should be considered as the main factor influencing their relative Raman intensities, while the EM enhancement greatly magnifies the CE effect on their SERS signals. The CE effect can be divided into two kinds of surface Raman scattering processes: (1) the chemical binding induced enhancement; and (2) the CT mechanism.

First, we concentrate on how the binding interaction influences the change in relative Raman intensities of the SERS spectra of Py.[14,32–35] Fig. 9(a) shows the simulated Raman spectra of free Py and Py interacting with Ag_4, Au_4 and Pt_5 clusters under an assumption that Raman signals are only affected by the binding interaction. As seen in Fig. 7(a) and 9(a), the observed spectrum of pure liquid Py can be reproduced well using the DFT calculation for free Py at the B3LYP/6-311+G**(C, N, H) level. This result clearly shows that there is a large difference in the relative intensity of the ν_1 and ν_{12} modes for Py–Ag_4, Py–Au_4 and Py–Pt_5. For these three model complexes, the strength of the binding interaction has an ascending order, Py–Ag_4 < Py–Au_4 < Py–Pt_5.[43,45] Because the binding interaction is the weakest in Py–Ag_4, the Raman spectrum of Py is expected to be the most similar to that of free Py. In Py–Au_4, the Raman intensity of the ν_{12} mode significantly decreases due to a strong bonding between Py and Au_4. For Py–Pt_5, the strong binding interaction leads to a decrease in the Raman intensity of the ν_{12} mode but enhances those of the ν_{6a}, ν_{8a} and ν_{9a} modes. This result agrees with the observed SERS spectra of Py adsorbed on the Pt electrode at the open circuit potential. If the Raman intensity of free Py is regarded as a reference, we define the enhancement factor as the ratio of the Raman intensities of the same vibrational mode in Py–Pt_5 to that in free Py. Thus, we can obtain the enhancement factors about 20 for the modes. This is comparable to the CT enhancement factor for Py adsorbed on a rough cobalt electrode.[6] It shows that the binding interaction is determined by both the property of the vibrational mode itself and the metals.

Second, one should pay attention to how the CT mechanism can influence the relative intensities of SERS spectra of Py on silver, *e.g.*, at the peak potential of the ν_1 mode. As seen in Fig. 7(b), the ν_{12} band weakens due to the participation of the CT mechanism, which is contributed by the electron transition from the Fermi level of Ag electrode to the unoccupied $3b_1$ or $2a_2$ orbitals (*e.g.*, see Fig. 8). The two excited states generally

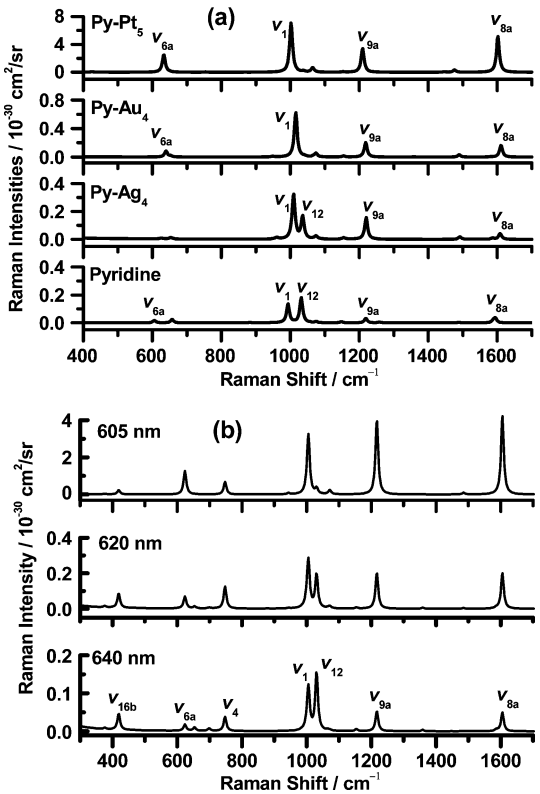

Fig. 9 Simulated Raman spectra of pyridine, pyridine interacting with Ag_4, Au_4 and Pt_5 clusters in the off-resonance-Raman scattering process (a), and pyridine interacting with Ag_2 in the pre-resonance-Raman scattering process (b).

have a small energy gap of about 0.5 eV.[43,44] Thus, both CT states may contribute simultaneously to the SERS signal of Py. Because we adopted a pre-resonance Raman scattering to investigate the CT mechanism, the low-lying photon-driven CT state plays an important role. The simulated spectra in Fig. 9(b) show that Raman signals of the ν_{6a}, ν_1, ν_{9a} and ν_{8a} modes are significantly enhanced when the resonance condition is satisfied. In comparison to the ν_1 mode, the Raman signal of the ν_{12} mode becomes weak, in good agreement with the observed spectra. This result can be interpreted by that the enhancement in the Raman intensities of different vibrational modes depends on the Huang–Rhys factor that measures the displacement of a normal coordinate of the adsorbed molecule at the excited and ground states in the CT process.

Although the vibrational modes will have a same electric transition dipole moment as well as the electronic damping constant when the excited CT state is a specific intermediate state in a resonance-Raman scattering process, the Huang–Rhys factors are different for the various modes. From our previous work, the Huang–Rhys factors of ν_{6a}, ν_1, ν_{8a} and ν_{9a} modes are 0.152, 0.309, 0.339 and 0.288, respectively.[13,46] These values is obviously larger than 0.035 for the ν_{12} mode and 0.001 for the in-plane C–H stretching, in agreement with the previous results.[47] Therefore, the CT mechanism enhances significantly the Raman signals of the former four modes. For the ν_{18a} and ν_{19a} modes, the CT enhancement effect is expected to be very small due to the small Huang–Rhys factor.

Therefore, one could interpret the unique spectral change for Py adsorbed on different electrode surfaces with a combined consideration of chemical interaction and CT mechanism. On the Ag surface CT is the main mechanism to cause a decrease in the relative Raman intensity of the ν_{12} mode with respect to the ν_1 mode. On the Cu and Au surfaces, a larger relative intensity of the ν_1 to ν_{12} modes can be interpreted as the synergetic effect of the chemisorption and the CT enhancement mechanism. For ν_{8a} and ν_{9a} modes, both the strong chemisorption and the CT mechanism enhance their Raman signals. The frequency shift and change of the SERS intensity of the vibrational bands should be closely associated with the interfacial electrochemical process.

4.2 Water and hydrogen adsorption on Pt, Pd and Au electrodes

Water is the most important solvent and plays vital roles in electrochemistry as the configuration and orientation of surface water can directly affect interfacial electrochemical processes. Clarifying the interfacial water at the microscopic level can greatly improve our fundamental understanding of the electrode/electrolyte interface, which is still an eternal issue in electrochemistry and surface sciences. SERS can not only avoid severe interference from the enormous bulk water (about 55 M) but also tremendously enhance the Raman signal of surface water. There have been some interesting SERS studies revealing the dependency of the structure of surface water on potentials, ions and pH. However, all these studies have almost been limited to coinage metals. Recently, we utilized a strategy of borrowing the SERS activity by chemically coating several atomic layers of a transition metal on the highly SERS-active Au nanoparticles. Using the high electromagnetic enhancement of the Au core to effectively boost the surface Raman signal of species on the shell metals, we have successfully observed the first SERS (also the first Raman) signal of surface water on Pt-group metals.[48] The SERS spectra obtained allow us to scrutinize the interfacial structure of water on these electrode surfaces and also to compare with the typical SERS-active substrates.

To obtain high quality SERS spectra of interfacial water, the Raman cell was placed in a vertical way so that the surface of the working electrode remained perpendicular, which can effectively avoid the accumulation of bubbles on the surface of electrode or optical window during the hydrogen evolution. Furthermore, for investigation of the SERS of water, it is really important to keep the solution free of impurities that may easily repel the water from the surface.

Fig. 10 shows potential-dependent SERS spectra of water adsorbed on Pt, Pd and Au surfaces in the potential region of the hydrogen evolution reaction, wherein the band at around 1615 cm^{-1} is the bending vibration of water. It should be emphasized that the SERS intensity of the bending vibration is just about the same as that of the stretching one. This is in clear contrast to the fact that the Raman intensity of the bending mode is normally about 20 and 100 times lower than that of the stretching mode for the bulk and gas water, respectively. The broad band at around 2000 cm^{-1} observed

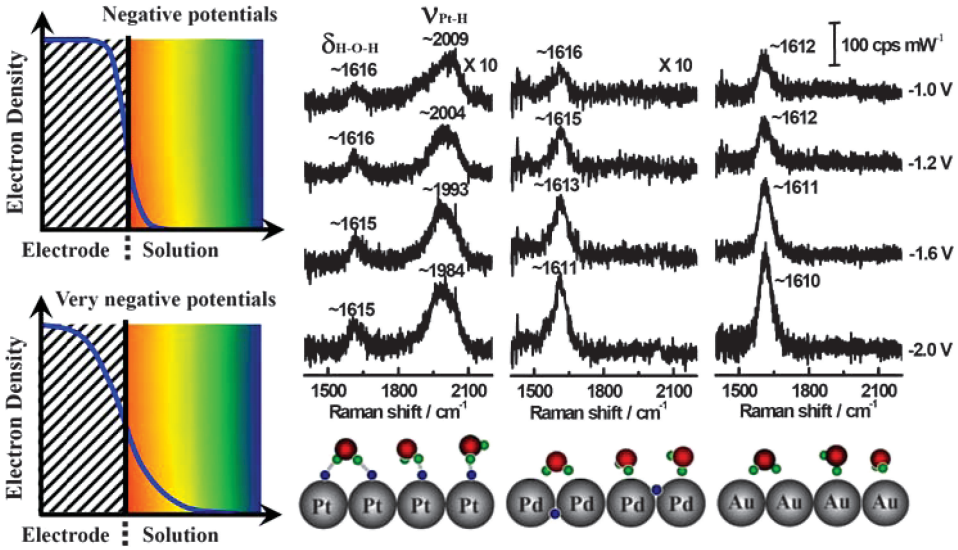

Fig. 10 SERS of water adsorbed on Pt, Pd and Au at negative potentials in 0.1 mol L^{-1} $KClO_4$ with the excitation wavelength of 632.8 nm (right top). The suggested models (right bottom) for the adsorbed water on different electrodes and the influence of potential on metal conduction electron are shown on the left.

only on the Pt surface is ascribed to the Pt–H stretching vibration.

For the O–H stretching vibration, the extent of the frequency shift with the applied potentials (*i.e.*, vibrational Stark effects) on Pt is significantly less than that on the Au and Pd electrodes. To account for the different spectral feature of water in the negative potential region, we proposed three adsorption models for the three metals.[48] It is of interest that the SERS signal of water is much stronger at the negative potentials than the PZC and further enhances with the negative movement of the potential, as seen in Fig. 10. This abnormal phenomenon could be explained by the influence of the electronic enhancement. The metal conduction electron has a high polarizability and the surface electronic tail penetrates into the solution to a distance of several angstroms at more negative potentials.[27] Under this condition, the surface water molecules are immersed in 'the electronic cloud' in addition to the local optical electric field, which could further enhance the SERS signal of the interfacial water. This work may shed light on the SERS study on the complicated mixture of EM field and electric field cross the double layer for further increasing the SERS activity.

4.3 Electrochemical reactions and electrode kinetics

By taking advantage of the high sensitivity provided by SERS effect, it becomes possible to obtain a full spectrum within milliseconds for monolayer species using a multichannel detector. This feature allows SERS to detect not only the adsorption/desorption behavior, but also the redox process of the surface species by providing direct identification of the adsorbed intermediates and/or products formed in multi steps. When combined with conventional electrochemical measurements, SERS can identify the intermediates and evaluate the reaction pathways of the electrochemical reaction. A good example of such type of study is the combined SERS and cyclic voltammetric study of nitrobenzene surface reaction on a SERS-active Au surface.[49] It is known that nitrobenzene can be reduced by three two-electron steps to form nitrosobenzene, phenylhydroxyamine and aniline:

$$C_6H_5NO_2 \xrightarrow{2e^-} [C_6H_5NO] \xrightarrow{2e^-} C_6H_5NHOH \xrightarrow{2e^-} C_6H_5NH_2$$

nitrosobenzene was not detected by analytical methods, it may be consumed by the chemical coupling reaction following the electrochemical reaction:

$$C_6H_5NO + C_6H_5NHOH \rightarrow C_6H_5N{=}N(O)C_6H_5$$

From the cyclic voltammograms of nitrobenzene in the sulfuric acid solution in Fig. 11(a), one can find a pair of peaks at 0.11 and −0.27 V of the reduction of nitrobenzene. The anodic peak at 0.33 V has been assigned to the formation of nitrosobenzene, and the cathodic peak at 0.30 V is from the reduction of nitrosobenzene to phenylhydroxyamine. The 30 mV separation independent of the scan rate indicates that the above pair of reaction is a reversible process. The SER spectra were acquired during the potential sweep for the reduction of nitrobenzene at the gold electrode, see Fig. 11(b). It can be seen that during the positive movement of the electrode potential, the band at 1330 cm^{-1} corresponding to the nitrobenzene decreases. Meanwhile, new bands located at 1146, 1388 and 1588 cm^{-1}, respectively grew up when the potential was negative of −0.11 V. Compared with the normal Raman and SER spectra of possible reaction products, these new peaks detected during the reduction present essentially the feature of nitrosobenzene. Correlated the voltammetric and SERS results, the peak at −0.11 V in the cyclic voltammogram can be assigned to the reduction of nitrobenzene to nitrosobenzene. This study provides a good example to combine electrochemical method and SERS to investigate the electrochemical reaction on the surface and to scrutinize the pathway and intermediates of the reaction.

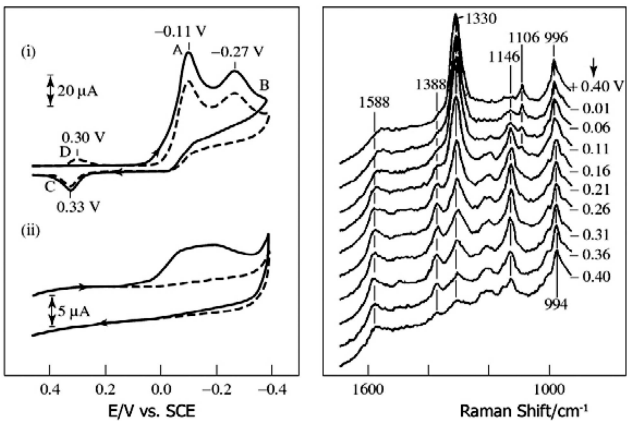

Fig. 11 (Left) Cyclic voltammograms (i) for 1 mM nitrobenzene in 0.1 mol L^{-1} H_2SO_4 at a gold electrode. Solid and dashed traces refer to the first and second consecutive cycles, respectively; (ii) for irreversibly adsorbed nitrobenzene in 0.1 mol L^{-1} H_2SO_4. Sweep rate: 100 mV s^{-1}. (right) Sequence of surface-enhanced Raman spectra obtained during linear sweep voltammetric reduction of nitrobenzene at a gold electrode. The potential sweep rate was 5 mV s^{-1}, negative-going from 0.4 V *vs*. SCE. The solution was 3×10^{-3} mol L^{-1} nitrobenzene in 0.1 mol L^{-1} H_2SO_4. Potentials indicated beside each spectrum are average values during the 5 s detector integration time. Excitation line: 647.1 nm. (Reproduced with permission from ref. 49. Copyright 1988, American Chemical Society.)

5 Prospective developments of EC-SERS

As has been shown EC-SERS is one of the most complex systems, which operates with the synergetic effect of SERS and electrochemistry. All EC-SERS-active systems must possess nanostructures and the SERS activity is critically dependent on the configuration and composition of nanostructures as well as the applied electrode potential, by which some new insights on the SERS phenomena can be gained. Electrochemistry appreciates SERS as a powerful tool to characterize surface molecules, which may provide the 'fingerprint' information of their molecular bonds and molecule–surface bond. However, so far the EC-SERS process still lacks a complete microscopic understanding, such as the SERS behavior of water in different potential regions. It is also necessary to further expand the substrate, surface, and molecule generalities of EC-SERS. We will briefly describe some future developments in terms of the EC-SERS substrate, method and theory.

Ordered nanostructured electrode surfaces

Most EC-SERS substrates prepared by electrochemical roughening procedures are generally ill-defined in size and shape. As a consequence, they are plagued practically by poor reproducibility. The main trend is to further develop some simple and effective methods to fabricate well-ordered nanostructured electrode surfaces by electrochemical and/or chemical method, such as template methods.[38,39] This will provide great opportunity for not only improving the reproducibility and optimizing the SERS activity of existing materials but also searching for a new generation of SERS materials, such as bi-metallic and alloy materials. The match between theory and experiment enables effective design of nanostructures tailored with the special size, shape and inter-particle spacing, which could possess radically suitable plasmon modes. It is advantageous to utilize the template method and nanoimprinting technique to reproducibly fabricate electrically conductive substrates with ordered spherical shapes or voids. In order to further expand the SERS generality of electrode materials, one could devise and then synthesize core–shell (or sandwiched) nanostructures, *e.g.*, consisting of a highly SERS-active metal and a non-SERS-active semiconductor or conducting polymer, which may extend the EC-SERS to semiconductor electrochemistry even the whole range of materials in electrochemistry.

Well-defined single-crystal electrode surfaces

It is highly desirable to extend the SERS substrate from the ill-defined surface to atomically flat and well-defined surfaces. This target is crucially important for surface science and electrochemistry. SERS obtained from atomically flat single-crystal surfaces will be greatly helpful for studying the orientation of adsorbates unambiguously and for comparing surface selection rules of conventional Raman spectroscopy and SERS.[50] Moreover, the well-defined single-crystal surface is completely different from the typical "SERS-active sites" including a wide variety of adatoms, ad-clusters and surface complexes. The former have well known electronic levels of metal or surface states, which are essential parameters for revealing the chemical mechanism, if it exists. Before the Raman instrumentation can improve the detection sensitivity up to the monolayer level, there could be two approaches to realize this goal in terms of new substrate and new method. It is now feasible to synthesize metal nanocrystals with well-defined facets. The most challenging issue is how to assemble these nanocrystals as a well-ordered structured electrode then how to extract the SERS signal solely from the facet instead of the crystal edge that may provide a stronger signal.

Electrochemical tip-enhanced Raman spectroscopy (EC-TERS)

In addition to the above-mentioned method for investigating the single-crystal surface, we should pay special attention to a new technique that may play a key role and find important application in electrochemistry, called tip-enhanced Raman spectroscopy (TERS). TERS combines Raman microscopy with scanning probe microscopy and works by placing a Au or Ag tip very close to a sample (1 to several nm). By illuminating the formed gap with a laser of suitable wavelength and polarization, the localized surface plasmons can be excited, which will produce a large increase of the electromagnetic field and up to six orders of magnitude increase of the Raman intensity of the sample underneath the tip. This enhancement makes it a reality to obtain the TERS signal of non-resonant molecules adsorbed on single-crystal Pt and Au surface and the molecular resolution topographic image.[51] A spatial resolution of 14 nm has been reported experimentally,[52] which makes it possible to reveal the role of terraces, steps, facets and different surface roughness during the adsorption process or in the course of chemical reactions. TERS may shed new light on the longstanding problem whether there

are any relations of SERS hot spot (active sites) and chemical active sites of electrodes. The major challenge in the application of TERS in electrochemistry is how to avoid or eliminate the distortion of the liquid layer to the optical systems and to avoid the adsorption of target molecules to the tip surface.

Probing electronic structures of adsorbates and electrode nanostructures

EC-SERS may also be applied to probe the energetic levels of the adsorbate or surface nanostructure by analyzing the potential dependent SERS intensity of different bands of the probe molecule. On the basis of the chemical enhancement mechanism,[15,46] one could apply the electrode potential and/or use the tunable laser to tune the incident photon energy to match the specific Raman resonance. EC-SERS may also provide a new way to detect the intermediate energy levels of surface species or surface complex during electrochemical reactions and processes. The pump–probe investigation with tunable excitation line could be applied for the purpose. Furthermore, the ultra-fast SERS and other surface spectroscopies such as femtosecond infrared spectroscopy can probably be combined for studying the SERS mechanism, especially for the detailed analysis of the photon-driven charge-transfer process in electrochemical systems. Since SERS, surface-enhanced infrared spectroscopy, surface-enhanced fluorescence spectroscopy and surface-enhanced sum frequency generation belong to a family of surface-enhanced optical spectroscopy, the combination of these techniques will allow a systematic assessment of the contribution of physical and chemical enhancement to SERS and ultimately for a comprehensive understanding of the SERS mechanism.[53]

Applications of EC-SERS in biosciences and biosensors

Shortly after its discovery, SERS was applied in the detection of biomolecules.[54] Recently, there is a growing interest in using "SERS reporter" technique that can significantly amplify the weak signal of the species to be detected using reporters with a strong Raman signal, for trace detection of molecule in solution and specific molecules in live cells or animals.[55] Up to date, there are only a few reports on using EC-SERS for biodetection, *e.g.*, detecting the electron transfer dynamics during the electrochemical redox process of cytochrome c by using time-resolved surface-enhanced resonance-Raman scattering. However, in these studies, the advantages of EC-SERS have not been fully exploited. As mentioned in the section 2, by properly controlling the electrode potential we can tune the surface enhancement to the maximum and the surface to a state suitable for biomolecule interaction, it will not only enhance the sensitivity of SERS but also the selectivity for biodetection. Furthermore, simultaneous detection by both SERS and EC method may provide additional information for the complex biosystems. Applying EC-SERS to biodetection by making full use of its advantage will be a very important direction and opportunity for EC-SERS with the growing demand of the limit of detection and higher selectivity for diagnostic techniques in biological and biomedical applications.

Theory of EC-SERS

There has been lack of a unified theory that can explain all the phenomena observed experimentally. Even for the individual mechanism, there are still some unsolved problems.[56] For instance, in the EM mechanism, how to correct the dielectric constant of nanoparticles and how the surface plasmon radiation competes with the other optical processes. Furthermore, one has to understand how the position and efficiency of the surface plasmon resonance will be affected when specific adsorption occurs or a potential is applied on the electrode surface. On the CE mechanism, the CT process involves in the coupling of the irregular and complicate metal surface, adsorbed molecules, and laser or other external sources. Till now, it still remains a problem to find out the detailed structure of the surface active sites of SERS. Although there are some reports on the existence of the direct or indirect photon-driven CT between the adsorbed molecule and the metal surface from the electron energy loss spectroscopy and the two-photon photoemission technique, it is still not persuasive whether the four-step or two-step CT processes really take place at the electrochemical interfaces or vacuum/metal interfaces.[57] Apparently, more evidence is necessary for confirming and then understanding the detailed process of the CT mechanism of SERS. Further effort both in experiment and theory is undoubtedly helpful for a complete understanding of SERS by a unified and simultaneous consideration of both EM and CE mechanisms in electrochemical systems.

In summary, through more than three decades of research effort by many groups including ours, EC-SERS has made some contributions to developments of SERS and spectroelectrochemistry. The latest advances relied mostly on developing various techniques for fabricating nanostructured electrode surfaces. There are good reasons to be optimistic that EC-SERS will become increasingly general and indispensable tools in fundamental studies and widespread applications. Along with developments in nanoscience, Raman spectroscopy and electrochemistry, many opportunities will emerge to enhance our understanding of SERS and to advance EC-SERS into a versatile and powerful tool for wide applications in SERS, electrochemistry and nanoscience.

Acknowledgements

This work has been possible by the continuous financial support of the Natural Science Foundation of China (Nos. 20433040, 10474082, 20573087 and 20673086), Ministry of Science and Technology (973 Program Nos. 2007CB815303 and 2007CB935603), Fok Ying Tung Foundation (101015), and the NCET projects of the Ministry of Education of China for B. R. (NCET-05-5664) and D. Y. W. Whenever the work from the authors' group is mentioned in the article, it is the great contribution of the self-motivated and hard working students, that should be acknowledged.

References

1 R. E. White, J. O' M. Bockris, B. E. Conway and E. Yeager, *Comprehensive Treatise of Electrochemistry*, Plenum Press, New York, 1984, vol. 8.

2 M. Fleischmann, P. J. Hendra and A. J. McQuillan, *Chem. Phys. Lett*., 1974, **26**, 163.
3 D. L. Jeanmaire and R. P. Van Duyne, *J. Electroanal. Chem*., 1977, **84**, 1.
4 M. G. Albrecht and J. A. Creighton, *J. Am. Chem. Soc*., 1977, **99**, 5215.
5 R. P. Van Duyne, in *Chemical and Biochemical Applications of Lasers*, ed. C. B. Moore, Academic Press, New York, 1979, vol. 4, p. 101.
6 Z. Q. Tian, B. Ren and D. Y. Wu, *J. Phys. Chem. B*, 2002, **106**, 9463.
7 Z. Q. Tian, B. Ren, J. F. Li and Z. L. Yang, *Chem. Commun*., 2007, 3514.
8 M. Fleischmann and I. R. Hill, in *Comprehensive Treatise of Electrochemistry*, ed. R. E. White, J. O. M. Bockris, B. E. Conway and E. Yeager, Plenum Press, New York, 1984, vol. 8, p. 373.
9 B. Pettinger, in *Adsorption at Electrode Surface*, ed. J. Lipkowski and P. N. Ross, VCH, New York, 1992, p. 285.
10 (*a*) S. Zou and M. J. Weaver, *Anal. Chem*., 1998, **70**, 2387; (*b*) S. Park, P. X. Yang, P. Corredor and M. J. Weaver, *J. Am. Chem. Soc*., 2002, **124**, 2428.
11 Z. Q. Tian and B. Ren, *Annu. Rev. Phys. Chem*., 2004, **55**, 197.
12 M. Moskovits, *J. Raman Spectrosc*., 2005, **36**, 485.
13 R. K. Chang and T. E. Furtak, *Surface Enhanced Raman Scattering*, Plenum Press, New York, 1982.
14 A. Otto, I. Mrozek, H. Grabhorn and W. Akemann, *J. Phys.: Condens. Matter*, 1992, **4**, 1143.
15 R. L. Birke and J. R. Lombardi, in *Spectroelectrochemistry – Theory and Practice*, ed. R. J. Gale, Plenum, New York, 1988, p. 263.
16 A. Otto, in *Light Scattering in Solid*, ed. M. Cardona and G. Guntherodt, Springer-Verlag, Berlin, 1984.
17 A. Wieckowski, in *Interfacial Electrochemistry*, ed. M. Dekker, New York, 1999.
18 D. Y. Wu, B. Ren, X. Xu, G. K. Liu, Z. L. Yang and Z. Q. Tian, *J. Chem. Phys*., 2003, **119**, 1701.
19 D. Y. Wu, M. Hayashi, S. H. Lin and Z. Q. Tian, *Spectrochim. Acta, Part A*, 2004, **60**, 137.
20 L. L. Zhao, L. Jensen and G. C. Schatz, *J. Am. Chem. Soc*., 2006, **128**, 2911.
21 S. A. Maier and H. A. Atwater, *J. Appl. Phys*., 2005, **98**, 011101.
22 Z. Q. Tian, Z. L. Yang, B. Ren, J. F. Li, Y. Zhang, X. F. Lin, J. W. Hu and D. Y. Wu, *Faraday Discuss*., 2006, **132**, 159.
23 Z. Q. Tian, Z. L. Yang, B. Ren and D. Y. Wu, Surface-Enhanced Raman Scattering-Physics and Applications, *Top. Appl. Phys*., 2006, **103**, 125.
24 U. Kreibig and M. Vollmer, *Optical Properties of Metal Clusters*, Springer, Berlin, 1995.
25 A. H. Ali and C. A. Foss, *J. Electrochem. Soc*., 1999, **146**, 628.
26 V. O. Santos, M. B. Alves, M. S. Carvalho, P. A. Z. Suarez and J. C. Rubim, *J. Phys. Chem. B*, 2006, **110**, 20379.
27 B. I. Lundqvist, O. Gunnarsson, H. Hjelmberg and J. K. Norskov, *Surf. Sci*., 1979, **89**, 196.
28 J. Gersten and A. Nitzan, *J. Chem. Phys*., 1980, **73**, 3023.
29 A. Otto, J. Billman, J. Eickmans, U. Erturk and C. Pettenkofer, *Surf. Sci*., 1984, **138**, 319.
30 A. Campion and P. Kambhampati, *Chem. Soc. Rev*., 1998, **27**, 241.
31 R. L. McCreery, *Raman Spectroscopy for Chemical Analysis*, John Wiley, New York, 2000.
32 K. Izutsu, *Electrochemistry in Nonaqueous Solutions*, Wiley-VCH, Weinheim, 2002.
33 Z. Q. Tian and B. Ren, in *Encyclopedia of Electrochemistry*, ed. P. Unwin, A. J. Bard and M. Stratmann, Wiley-VCH, Weinheim, 2003, vol. 3, p. 572.
34 P. Gao, D. Gosztola, L.-W. H. Leung and M. J. Weaver, *J. Electroanal. Chem*., 1987, **233**, 211.
35 Z. Liu, Z. L. Yang, L. Cui, B. Ren and Z. Q. Tian, *J. Phys. Chem. C*, 2007, **111**, 1770.
36 G. Frens, *Nat. Phys. Sci*., 1973, **241**, 20.
37 B. Wiley, Y. Sun and Y. Xia, *Acc. Chem. Res*., 2007, **40**, 1067.
38 K. A. Willets and R. P. Van Duyne, *Annu. Rev. Phys. Chem*., 2007, **58**, 267.
39 S. Mahajan, M. Abdelsalam, Y. Sugawara, S. Cintra, A. E. Russell, J. J. Baumberg and P. N. Bartlett, *Phys. Chem. Chem. Phys*., 2007, **9**, 104.
40 D. Y. Wu, B. Ren, Y. X. Jiang, X. Xu and Z. Q. Tian, *J. Phys. Chem. A*, 2002, **106**, 9042.
41 S. Haq and D. A. King, *J. Phys. Chem*., 1996, **100**, 16957.
42 M. Moskovits and D. P. Dilella, *J. Chem. Phys*., 1980, **73**, 6068.
43 D. Y. Wu, M. Hayashi, C. H. Chang, K. K. Liang and S. H. Lin, *J. Chem. Phys*., 2003, **118**, 4073.
44 J. A. Creighton, in *Progress in Surface Raman Spectroscopy: Theory, Techniques & Applications*, ed. Z. Q. Tian and B. Ren, Xiamen, Xiamen University Press, 2000, p. 11.
45 D. Y. Wu, B. Ren and Z. Q. Tian, *Isr. J. Chem*., 2006, **46**, 317.
46 M. T. Lee, D. Y. Wu, Z. Q. Tian and S. H. Lin, *J. Chem. Phys*., 2005, **122**, 094719.
47 J. F. Arenas, I. Lopez-Tocon, J. C. Otero and J. I. Marcos, *J. Phys. Chem*., 1996, **100**, 9254.
48 Y. X. Jiang, J. F. Li, D. Y. Wu, Z. L. Yang, B. Ren, J. W. Hu, Y. L. Chow and Z. Q. Tian, *Chem. Commun*., 2007, 4608.
49 P. Gao, D. Gosztola and M. J. Weaver, *J. Phys. Chem*., 1988, **92**, 7122.
50 A. Bruckbauer and A. Otto, *J. Raman Spectrosc*., 1998, **29**, 665.
51 X. Wang, Z. Liu, M. D. Zhuang, H. M. Zhang, X. Wang, Z. X. Xie, D. Y. Wu, B. Ren and Z. Q. Tian, *Appl. Phys. Lett*., 2007, **91**, 101105.
52 A. Hartschuh, E. J. Sanchez, X. S. Xie and L. Novotny, *Phys. Rev. Lett*., 2003, **90**, 095503.
53 R. Aroca, *Surface-enhanced Vibrational Spectroscopy*, John Wiley & Sons, Ltd., Chichester, 2006.
54 T. M. Cotton, *Adv. Spectrosc*., 1988, **16**, 91.
55 X. Qian, X. H. Peng, D. O. Ansari, Q. Yin-Goen, G. Z. Chen, D. M. Shin, L. Yang, A. N. Young, M. D. Wang and S. Nie, *Nat. Biotechnol*., 2008, **26**, 83.
56 J. R. Lombardi and R. L. Birke, *J. Chem. Phys*., 2007, **126**, 244709.
57 C. D. Lindstrom and X. Y. Zhu, *Chem. Rev*., 2005, **106**, 4281.